New Pressure-Swing Distillation for Separating Pressure-Insensitive Maximum Boiling Azeotrope via Introducing a Heavy Entrainer: Design and Control

ARTICLE *in* INDUSTRIAL & ENGINEERING CHEMISTRY RESEARCH · MAY 2013

Impact Factor: 2.59 · DOI: 10.1021/ie400274d

7 AUTHORS, INCLUDING:

Li Weisong
Tianjin University
9 PUBLICATIONS **41** CITATIONS

SEE PROFILE

I&EC research
Industrial & Engineering Chemistry Research

Article

pubs.acs.org/IECR

New Pressure-Swing Distillation for Separating Pressure-Insensitive Maximum Boiling Azeotrope via Introducing a Heavy Entrainer: Design and Control

Weisong Li,[†] Lei Shi,[†] Baoru Yu,[‡] Ming Xia,[†] Junwen Luo,[†] Haochun Shi,[†] and Chunjian Xu[†,*]

[†]State Key Laboratory of Chemical Engineering, Chemical Engineering Research Center, and School of Chemical Engineering and Technology, Tianjin University, Tianjin 300072, China

[‡]East China Engineering Science and Technology Co., Ltd., Hefei 230024, China

ABSTRACT: In this work, the pressure-swing distillation process is extended to separate the pressure-insensitive binary azeotropes by using suitable entrainers. Design and control of new pressure-swing distillation for separating pressure-insensitive maximum boiling phenol/cyclohexanone azeotrope using acetophenone as a heavy entrainer are investigated using Aspen Plus and Aspen Dynamics. Rigorous steady-state simulations are run for both fully and partially heat-integrated processes and a comparison of these two configurations is made. It is revealed that the partially heat-integrated process is more competitive than the fully heat-integrated one from the economical viewpoint. Two temperature control structures and one composition/temperature cascade control scheme are proposed to handle the feed flow rate and feed composition disturbances. It is indicated that the column operating at higher pressure cannot be perfectly controlled by the two temperature control schemes because of the existence of an intermediate nonkey component. A composition/temperature cascade control structure is proposed to cope with this control problem and a robust control is achieved.

1. INTRODUCTION

Phenol, also called carbolic acid, is widely used in the production of various chemical products such as resins, dyes, and pharmaceuticals. Traditionally, phenol is mainly obtained by the three-step Hock process with acetone as coproduct.[1−3] In recent years, market demand for acetone has decreased in contrast to the increasing need for phenol. To seek an alternative for phenol production, a one-pot synthesis from cyclohexylbenzene has been reported with cyclohexanone as the byproduct.[3,4] Cyclohexanone is the main intermediate in producing nylon, caprolactam, adipic acid, etc. and is also widely used as an excellent solvent in chemical industry. The one-pot synthesis is very attractive and promising, and shall be realized by industry before long.

The problem remains is how to separate the phenol/cyclohexanone mixture into the respective pure products. Highly pure phenol is needed when phenol is used for making pharmaceuticals or dyes, and cyclohexanone also needs to be purified. However, phenol and cyclohexanone form a maximum boiling azeotrope at atmospheric pressure with about 72 wt % phenol, and this azeotrope is pressure-insensitive. Thus a phenol/cyclohexanone mixture cannot be separated completely by a simple distillation process. The separation of azeotropic mixtures has been extensively studied in the literature. Many distillation techniques, including azeotropic distillation, extractive distillation, pressure-swing distillation and salt-addition distillation, have been proposed or applied in industry to separate azeotropes.[5−7]

Most of the literatures published focus on the separation of minimum boiling azeotropes. The investigation of the design for a maximum boiling azeotropic system is very limited. In the past decade, Lang[8,9] investigated the assessment of the feasibility of extractive distillation in a batch rectifier and extended it to the separation of maximum boiling azeotropes with continuous entrainer feeding. The rigorous simulation results verified that better separation can be achieved by batch extractive distillation (BED) rather than by the traditional solvent-enhanced batch distillation (SBD). Lelkes[10] investigated the separation of maximum boiling chloroform/ethyl acetate mixture using 2-chlorobutane as the intermediate boiling entrainer in both the BED and SBD systems. However, chloroform with entrainer and ethyl acetate-free rather than pure chloroform is obtained in both BED and SBD processes. Kotai and co-workers[11,12] also studied the separation of minimum/maximum boiling azeotropes in the BED process by feasibility studies and rigorous simulations, the maximum boiling acetone/chloroform mixture was separated in a liquid bypass version of a middle vessel column (MVC) by using toluene as an entrainer. It was proved that MVC is suitable for the BED separation of maximum azeotropes. However, the MVC is much more difficult to operate than a traditional batch rectifier (BR) because of its high degree of freedom. Batch distillation is only preferable to continuous distillation when there is a frequent variation in the composition and quantity of the mixture to be separated.

In the literature, pressure-swing distillation is often mentioned as an alternative process to the widely applied azeotropic or extractive distillation. Repke[13] investigated the separation of a minimum boiling acetonitrile/water mixture in the batch process by rigorous simulation and pilot-plant experiments. Modla and Lang[14] explored the separation of minimum and maximum boiling azeotropes in different batch configurations

Received: January 24, 2013
Revised: April 25, 2013
Accepted: May 13, 2013
Published: May 13, 2013

dx.doi.org/10.1021/ie400274d | *Ind. Eng. Chem. Res.* 2013, 52, 7836−7853

(such as rectifier, stripper, MVC, double column batch rectifier, and double column batch stripper) by feasibility studies and rigorous simulations. Furthermore, Modla and coauthors[15,16] proposed a classification of residue curve maps (RCM) for pressure-swing batch distillation and they also investigated the separation of a ternary system in a pressure-swing batch process. The continuous pressure-swing distillation without adding a third separating agent for separating binary homoazeotropes has been carefully studied by Yu, Luyben, and Muñoz et al.[6,17−19] However, this so-called pressure-swing distillation is only applicable to the separation of the azeotrope whose composition can be shifted substantially by changing system pressure, that is, a pressure-sensitive azeotrope. Knapp and Doherty[20] proposed a new pressure-swing distillation process for separating homoazeotropes. They proposed that the pressure-swing distillation can be extended to separate a broader class of pressure-insensitive azeotropes with a suitable pressure-swing entrainer. The entrainer causes distillation boundaries to move in one of three ways: (i) the entrainer forms no azeotropes at atmospheric pressure, but new pressure-sensitive azeotrope(s) appear(s) when the pressure changes; (ii) the entrainer forms one or more new azeotropic mixtures whose composition(s) changes rapidly with pressure; (iii) the entrainer forms one or more azeotropes at atmospheric pressure, but the azeotropes disappear as the pressure is changed. In addition, the procedures to screen the potential pressure-swing entrainers were also presented. In this work, we will apply this new pressure-swing distillation to the separation of a maximum boiling phenol/cyclohexanone mixture via introducing a suitable entrainer.

It is of great importance to select a suitable entrainer for this new pressure-swing distillation process. Heuristic methods and a computer aided molecular design (CAMD) method based on a genetic algorithm for entrainer selection have been extensively studied in the literature.[21−23] The entrainer screening procedure proposed by Foucher[21] requires only a knowledge of boiling temperatures and approximate compositions of any azeotropes. In most cases, the structure of simple distillation residue curve maps (RCM) for ternary mixtures can be uniquely determined by this procedure, and in no time the feasible entrainers can be identified. In our paper, the entrainer screening procedure proposed by Foucher is employed to select a suitable entrainer, and the feasibility of this new pressure-swing distillation is demonstrated using the RCM.

Chemical process design is creative and challenging. It includes problem assessment, process creation, evaluation, optimization, and plantwide controllability assessment.[24] Commercial process simulators such as Aspen Plus and Aspen Dynamics are frequently used to aid the steady-state design and dynamic simulations. The cost of the equipment and other costs related to the capital investment are of significant importance in selecting design alternatives. Douglas[25] proposed that total annual costs (TAC) could be used as the objective function to screen optimal designs among feasible alternatives, and a summary of equipment cost and utilities costs were presented in his book. TAC has been frequently used to evaluate different designs in the literature published.[5,6,26]

The purpose of this paper is to develop a new pressure-swing distillation system via introducing a suitable entrainer to achieve the separation of phenol/cyclohexanone mixture, with special focus on the design and control of this new process. Since the columns in the pressure-swing distillation process are being operated at different pressures, heat-integrated flowsheets are introduced to conserve energy consumption and reduce fixed capital investment. For one thing, both fully and partially heat-integrated flowsheets are considered and the optimum design of them based on TACs are compared to obtain the more economically competitive process. For the other thing, several control structures are proposed to effectively stabilize this optimum design.

2. STEADY-STATE DESIGN

2.1. Design of the New Pressure-Swing Distillation Process. Phenol and cyclohexanone form a pressure-insensitive maximum boiling azeotrope with 72.01 wt % phenol at 101.3 kPa with maximum boiling point of 184.5 °C, therefore it is hard to separate this mixture into two pure components via conventional pressure-swing distillation. Fortunately, as pointed out by Doherty,[20] the introduction of a suitable heavy entrainer would make this separation possible. This new pressure-swing process is simulated with the following data: the feed composition is 70/30 wt % phenol/cyclohexane and the flow rate is 3000 kg/h, with annual working time of 8000 h. The two product specifications are both specified as 99.9 wt %.

2.1.1. Entrainer Selection. The heuristic entrainer screening procedure proposed by Foucher[21] was employed to select the entrainers for separating phenol/cyclohexanone mixtures. By searching the Azeotropic Data,[27] we found that acetophenone and benzaldehyde would be the potential heavy entrainers. Both of them form maximum boiling azeotropic mixtures with phenol at atmospheric pressure. The maximum boiling points of phenol/benzaldehyde and phenol/acetophenone are 186.0 and 202.8 °C, respectively. The azeotropic compositions of these two azeotropes change rapidly with pressure, and the phenol concentration in the azeotropes increases with decreasing system pressure. However, the temperature difference between the boiling points of phenol/cyclohexanone and phenol/benzaldehyde azeotropes is only 1.5 °C. It means that benzaldehyde may not be a good heavy entrainer in this regard. In addition, benzaldehyde can be easily oxidized to benzoic acid which will act as an impurity in the products. Therefore, acetophenone is chosen as the heavy entrainer for our distillation process.

2.1.2. Property Package. The accuracy of simulated results strongly depends on the quality of physical property model parameters.[19] The Local Composition Models such as Wilson, NRTL, and UNIQUAC can describe the nonideality of the liquid phase. However, with the built-in binary interaction parameters in Aspen Plus, the three models could not predict the azeotropes precisely. Therefore, the binary interaction parameters for each model, obtained using "Data Regression" function in Aspen Plus with the experimental vapor−liquid equilibrium data,[28,29] are employed to predict azeotropes. Since the predicted azeotropic compositions of phenol/cyclohexanone and phenol/acetophenone fit well with the experimental values published in Azeotropic Data,[27] the UNIQUAC model with the regressed interaction parameters is competent to describe the liquid−vapor equilibrium of the phenol/cyclohexanone/acetophenone ternary system. The regressed binary interaction parameters for the UNIQUAC model are shown in Table 1.

2.1.3. Process Synthesis Using RCM Analysis. As expected, the phenol/cyclohexanone system is quite pressure-insensitive, whereas the phenol/acetophenone system shows a large shift in azeotropic composition as pressure changes. The phenol/acetophenone azeotropic point disappears at about 200 kPa. Thus we reach to an idea that introducing a heavy entrainer acetophenone can drag phenol into the bottoms of a distillation column in the form of pressure-sensitive phenol/acetophenone mixture, while the almost pure cyclohexanone is obtained in distillate.

dx.doi.org/10.1021/ie400274d | Ind. Eng. Chem. Res. 2013, 52, 7836−7853

Table 1. The Regressed Binary Interaction Parameters for the UNIQUAC Model

	phenol (i) / cyclohexanone (j)	phenol (i) / acetophenone (j)
A_{ij}	−0.96360	−9.35564
A_{ji}	0.29064	44.70417
B_{ij}/K	528.76141	40.51416
B_{ji}/K	−3.69289	−1738.79974
C_{ij}	0	1.56973
C_{ji}	0	−6.70282

The bottoms phenol/acetophenone mixture is then further separated in another column via pressure swing. This new pressure-swing distillation flowsheet is given in Figure 1.

To clearly describe this new pressure-swing distillation, RCM is used to evaluate the feasibility of this process. The RCM for the phenol/cyclohexanone/acetophenone ternary system at 3 and 200 kPa are shown in Figure 2a,b. In the RCM, there is a distillation boundary running from the phenol/cyclohexanone azeotrope to the phenol/acetophenone azeotrope at 3 kPa, putting the desired phenol and cyclohexanone products into two different distillation regions. The phenol/cyclohexanone azeotrope is pressure-insensitive, whereas the phenol/acetophenone azeotrope moves toward the acetophenone vertex with increasing column pressure. By 200 kPa the phenol/acetophenone azeotrope has moved to acetophenone vertex, ceasing to exist and causing the distillation boundary to move significantly. Thus a choice is to use the new pressure-swing distillation to purify cyclohexanone in a sub-atmospheric column and phenol in a column operating at 200 kPa (or a higher pressure).

As seen from the RCM in Figure 2c, the blue lines represent the material balance relationship that is based on lever-arm principle. In the low-pressure column (LPC), the total feed point F1 corresponds to a fresh feed F with a entrainer stream Recycle, F1 is separated into relatively pure cyclohexanone product D1 and bottoms stream B1. The bottoms stream B1 is essentially a binary phenol/acetophenone mixture. Then, B1 is to be separated in a high-pressure column (HPC). In the HPC, phenol goes overhead in the distillate D2, while the acetophenone stream (B2) descends into the bottoms, and then is recycled back to the LPC. To balance the tiny loss of the entrainer, a makeup stream of

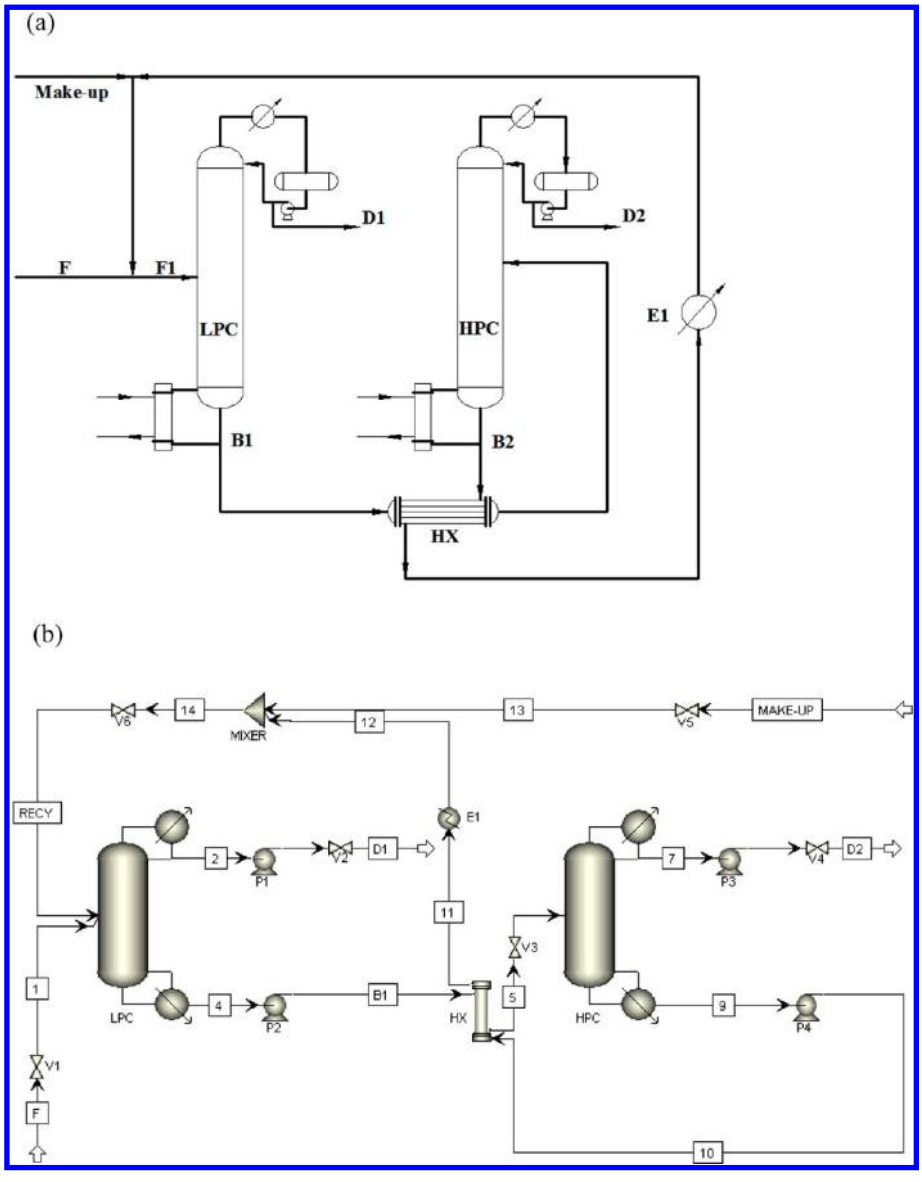

Figure 1. (a) Sketch of the new pressure-swing distillation process. (b) Process flow diagram implemented in Aspen Plus.

dx.doi.org/10.1021/ie400274d | *Ind. Eng. Chem. Res.* 2013, 52, 7836−7853

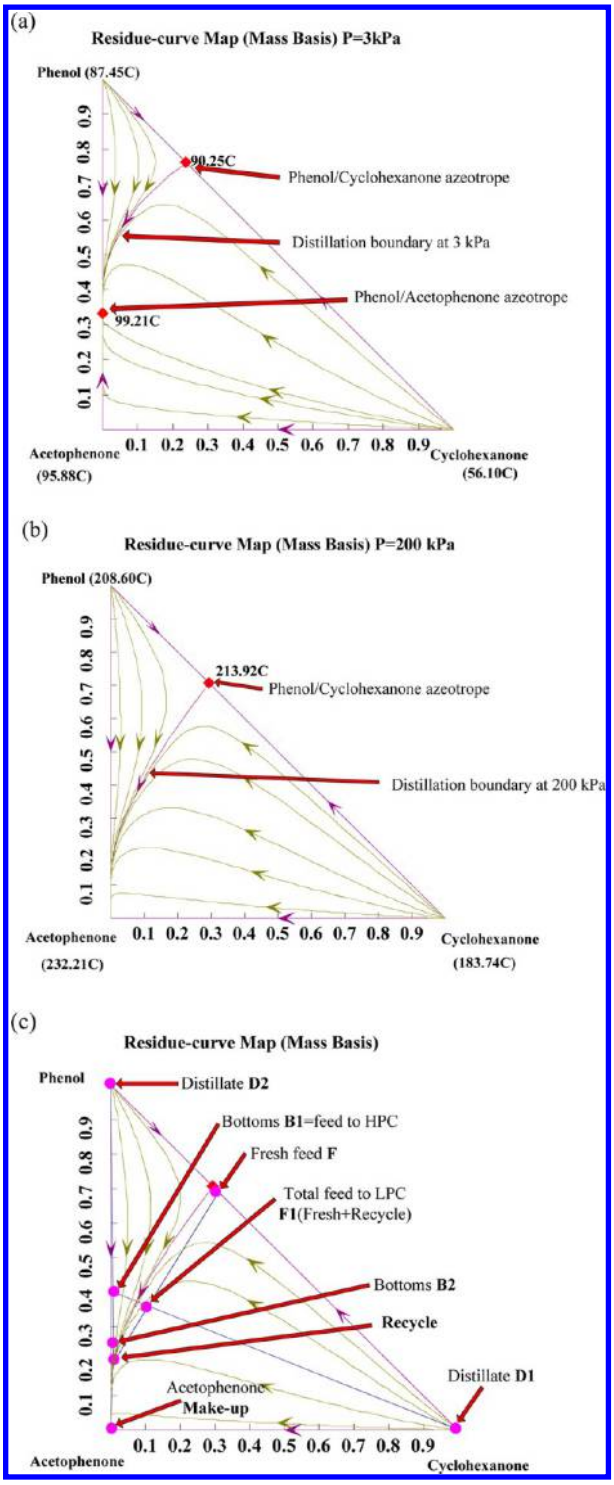

Figure 2. Residue curve maps for the cyclohexanone/phenol/acetophenone system: (a) residue curve map at 3 kPa, (b) residue curve map at 200 kPa, and (c) process feasibility analysis using the RCM.

acetophenone (Make-up) is added into the system. Note that the distillation boundary showed in Figure 2a is crossed with increasing system pressure. The RCM analysis proves that it is feasible to develop such a pressure-swing distillation for separating such a phenol/cyclohexanone mixture with acetophenone as a heavy entrainer.

In addition, B1 enters the HPC after being preheated by B2 through a heat exchanger HX for energy conservation, while B2 is further cooled by exchanger E1 before recycling to the LPC.

2.2. Preliminary Simulation. To begin the steady-state design, the operating pressures of the LPC and HPC (P_1 and P_2) are preliminarily set at 3 and 200 kPa, respectively. The composition in the LPC bottoms stream is set to be 31/69 wt % phenol/acetophenone, which is 2.12 wt % away from the corresponding azeotropic composition. When the flow rate of recycle stream (S) is given, the corresponding composition of the recycle stream can be easily determined by the following equation that is based on material balance.

$$\frac{x_{\text{phenol}}\cdot S + 70\ \text{wt}\,\%\cdot F}{(1 - x_{\text{phenol}})\cdot S} = \frac{31\ \text{wt}\,\%}{69\ \text{wt}\,\%} \quad (1)$$

where x_{phenol} and $(1 - x_{\text{phenol}})$ are the mass fractions of phenol and acetophenone in the recycle stream, respectively. F and S are the mass flow rates of the fresh feed F and the recycle stream, respectively. According to eq 1, the flow rate of the recycle stream is minimal when the recycle stream is pure acetophenone, and the minimum flow rate of the recycle stream (S_{min}) is 4674.19 kg/h.

A preliminary rigorous simulation is implemented with the RadFrac in Aspen Plus. We assume that the LPC and HPC have a total of 35 and 50 stages with an initial reflux ratio of 4.9 and 5, respectively. The flow rate of the recycle stream is 8000 kg/h with the corresponding acetophenone composition of 87.11 wt % which is calculated by eq 1. The fresh feed and the recycle stream are fed on stages 7 and 8 in the LPC, respectively, and the feed stage of the HPC is stage 20.

The distillate rate of the LPC (D_1) is varied to obtain 99.9 wt % cyclohexanone using a "Design spec/Vary" function in Aspen Plus and the reflux ratio of the HPC (RR_2) is manipulated to obtain 99.9 wt % phenol using the other "Design spec/Vary" function. The recycle stream is cooled to 50 °C which permits the use of cooling water. The stream B1 is heated to 180 °C by stream B2 and then fed to the HPC. The efficiency of all pumps is assumed to be 0.70.

The simulation results show that the temperature difference between the HPC condenser and the LPC reboiler is about 70 °C, and it indicates the possibility of heat integration between the two columns. Moreover, the reboiler duties are 1093.2 kW for the LPC and 2007.1 kW for the HPC, and the condenser duties are 677.9 kW for the LPC and 1670.2 kW for the HPC. It means that the heat-integrated process is feasible and this would reduce the fixed capital investment and energy consumption by a large margin.[30]

2.3. Optimization. Both full and partial heat integration are investigated in this paper. For the fully heat-integrated process, neat operation can be achieved without an auxiliary reboiler or condenser. However, the preliminary rigorous simulation results indicate that the condenser duty of the HPC is much greater than that of the LPC reboiler. To achieve neat operation, the LPC column vessel and reboiler heat transfer area would be much larger than actually required, resulting in larger fixed capital investment (FCI). So the partially heat-integrated process might be more attractive from the economical viewpoint. In the view that cooling water is much cheaper than a thermal system, as well as the negligible pump power compared with the heat duties of the reboilers, the HPC reboiler heat input QR_2 is employed as a reference variable to perform the partial optimization.

Design variables and optimization variables must be specified in the optimization. The temperature, pressure, flow rate, and composition of feed have already been specified, and the quality requirements of the two distillate products are selected as the

dx.doi.org/10.1021/ie400274d | Ind. Eng. Chem. Res. 2013, 52, 7836−7853

design variables. In each optimization, the number of stages and operating pressure are fixed. In contrast, the flow rate of the recycle stream (S), the reflux ratios of the two columns (RR_1 and RR_2), feeding locations(N_{F1}, N_{F2}, N_{FR}) of the feed streams and the recycle stream can be used as the optimization variables to minimize the HPC reboiler duty QR_2.

For a specific design, several alternatives that meet the design objective will be screened in conceptual design stage. Total annual cost (TAC) has been extensively used in screening chemical process design. After the TAC for each alternative is estimated, the design with the minimal TAC is achieved as the optimum design. The following objective function is used as the economical evaluation criteria.[19]

$$\text{TAC}\ (10^3\$/\text{year}) = C_v + i_r \times \text{FCI} \quad (2)$$

where C_v is the process variable costs, mostly utilities consumption (thermal system, cooling water, and electricity); FCI is the fixed capital investment; i_r is the fixed capital recovery rate applied to FCI and it is assumed to be 0.3 here.

Major pieces of equipment in this process are the two column vessels (including column internals, such as structured packing), reboilers, condensers, and the two heat exchangers. Small items such as pumps, valves, mixer, and the reflux drums are seldom significant at the conceptual design stage. The structured packing *Mellapak 250Y* developed by *Sulzer* is used in this process for the high throughput, low pressure drop, good separation efficiency, and small scale-up effect.[31] The "packing sizing" function in Aspen Plus is employed to size the column vessel. We specify the height equivalent to a theoretical plate (HETP) to be 0.4 m. To prevent the corrosion caused by phenol, all the column vessels (including the structured packing) and heat exchangers are made of stainless steel. The heat transfer areas for the condensers, reboilers, and heat exchangers are determined by using the overall heat transfer coefficient and a differential temperature driving force. The overall heat transfer coefficients recommended by Luyben[32] are 0.852 kW/(K·m^2) for the condensers and heat exchangers and 0.568 kW/ (K·m^2) for the reboilers, respectively. The cost estimation program *CAPCOST* involved in Turton's book[33] is used to estimate all the major equipment costs.

The utility costs are calculated in terms of the heat duties of reboilers, condensers, heat exchangers, and the power of all the pumps. Suppose that a moderate high thermal system (up to 330 °C) and 30 °C cooling water are available in the plant. The utility prices taken from *CAPCOST* are listed in Table 2.

Table 2. Utility Prices

utility	price ($/GJ)
moderate high thermal system (up to 330 °C)	12.33
cooling water (30 °C)	0.354
electricity (110−440 V)	16.8

2.3.1. Optimization for the Partially Heat-Integrated Process. In the partially heat-integrated process, the operating pressures of the LPC and HPC (P_1 and P_2) are initially fixed at 3 and 200 kPa, respectively. The recycle stream and the HPC feeding stream temperatures are set to be 50 and 180 °C, respectively. With the LPC reflux ratio RR_1 and HPC distillate rate D_2 fixed in each case, there are two variables being varied (D_1 and RR_2) to drive the two product compositions to their desired specifications. To find the best configurations for the partially heat-integrated process, the recycle streamflow rate (S), total stages of the LPC and HPC (N_1 and N_2), feeding locations (N_{F1}, N_{FR} and N_{F2}), and the LPC reflux ratio RR_1 need to be optimized. Since so many design variables need to be optimized, a calculation sequence is introduced to facilitate the optimization. The sequential iterative optimization procedure of the partially heat-integrated process is clearly demonstrated in Figure 3.

With the procedures presented in Figure 3, we started the optimization with 35 and 40 stages (using Aspen notation) in the LPC and HPC, respectively. Since the LPC bottoms stream is essentially a mixture of phenol and acetophenone, an extremely small amount of cyclohexanone could greatly affect the energy consumption of the HPC. Therefore, we first investigated the interaction between the LPC and HPC with reference to the cyclohexanone composition in the LPC bottoms stream. In the LPC, the cyclohexanone composition in the bottom stream is closely related to RR_1 with S fixed. A serial of simulations were carried out with various RR_1 when S is fixed at 8000 kg/h; the effects of RR_1 on the cyclohexanone composition in the LPC bottoms and the HPC reboiler duty are illustrated in Figure 4. As seen in Figure 4, the cyclohexanone composition decreases slowly with the increasing RR_1, and it can be easily maintained at a very low level (lower than 0.03 wt %). However, the HPC reboiler duty QR_2 decreases sharply with increasing RR_1, and it shows a plateau when RR_1 is larger than 5. This indicates that an excessive large RR_1 does not help to reduce the cyclohexanone impurity in B1 and energy consumption. Since a larger RR_1 means larger column vessel and reboiler for the LPC, this results in a higher fixed capital investment for the LPC. So, there may exist an optimum RR_1 that gives the minimum TAC with a reasonable low level of cyclohexanone impurity in the LPC bottoms stream when S is given.

Moreover, the performance (such as FCI, energy consumption, ect.) of this process can be influenced by the recycle streamflow rate S. According to eq 1, a smaller S means a higher purity of acetophenone in the recycle stream, and it would require a higher HPC reflux ratio to facilitate the separation. This results in a higher energy consumption. On the other hand, A larger S means larger liquid handling capacities for both columns, this results in a higher fixed capital investment. Thus, there also exists an optimum S. The effects of S and RR_1 on the TAC are illustrated in Figure 5. It is obvious that the minimum TAC is $\$1.186 \times 10^6$ when RR_1 is 4.6 with S fixed at 8000 kg/h.

The next step is to determine the total number of stages in the LPC (N_1). Intuition would lead us expect that there is an optimum N_1 that gives a minimum TAC with N_2 fixed at 40. The effect of N_1 on TAC is shown in Figure 6, in which each point corresponds with an optimal design (i.e., minimum TAC). It is indicated that the optimum N_1 is 35 with the minimum TAC of $\$1.186 \times 10^6$ per annum.

The final step for the optimization of this partially heat-integrated process is to optimize the number of stages in the HPC. The effect of N_2 on TAC is presented in Figure 7. It is obvious that the optimum N_2 is 50 with the minimum TAC of $\$1.173 \times 10^6$ per annum.

2.3.2. Optimization for the Fully Heat-Integrated Process. In the fully heat-integrated process, no auxiliary condenser is used. The only heat input is the HPC reboiler duty QR_2. To achieve this "neat" configuration, "flowsheet design spec" feature in Aspen Plus is used , and RR_1 is manipulated to make the LPC reboiler duty QR_1 and the HPC condenser duty QC_1 equal in magnitude but opposite in sign. The LPC distillate D_1 and the HPC reflux ratio RR_2 are also adjusted to meet the two product specifications. Thus, the optimization sequence for the fully heat

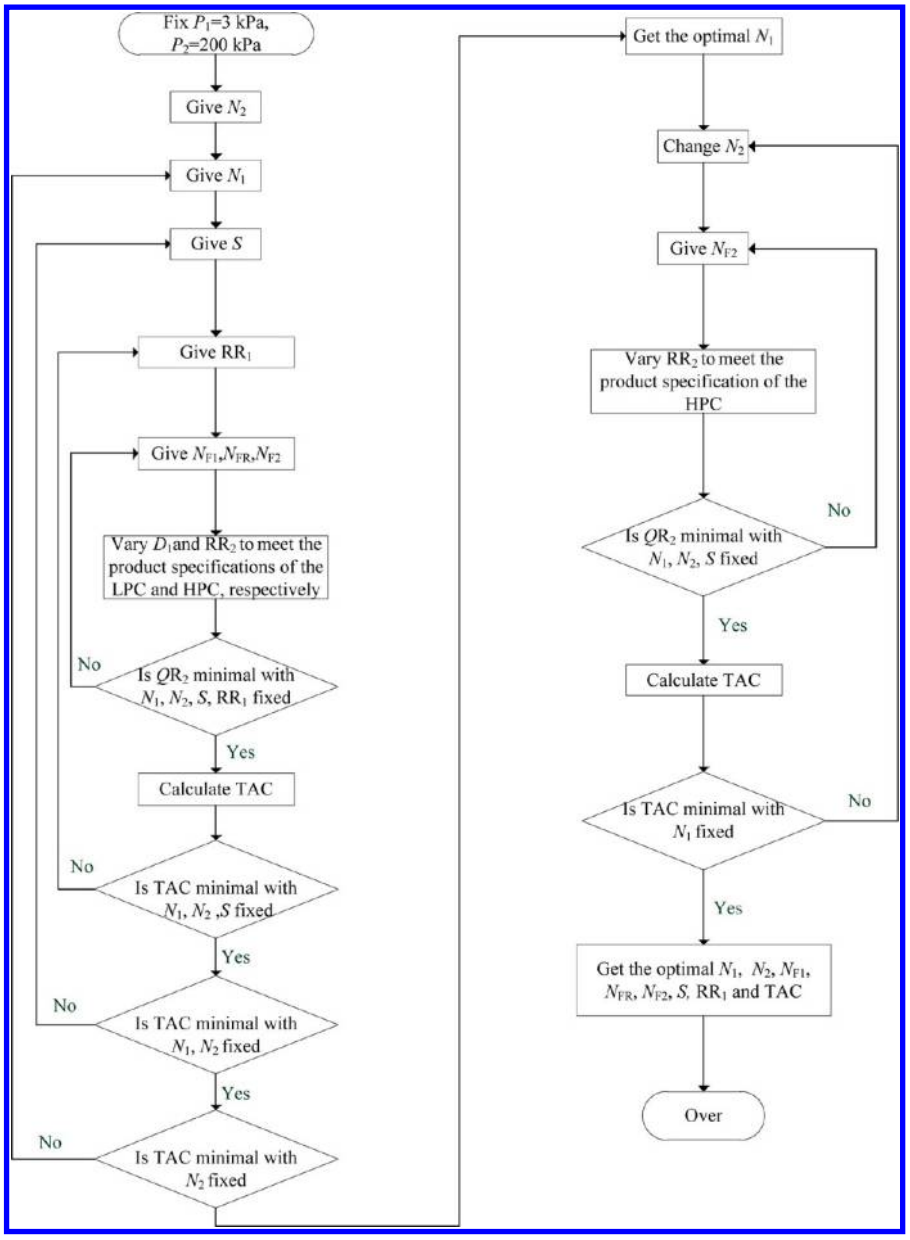

Figure 3. Sequential iterative optimization procedure for the partially heat-integrated process.

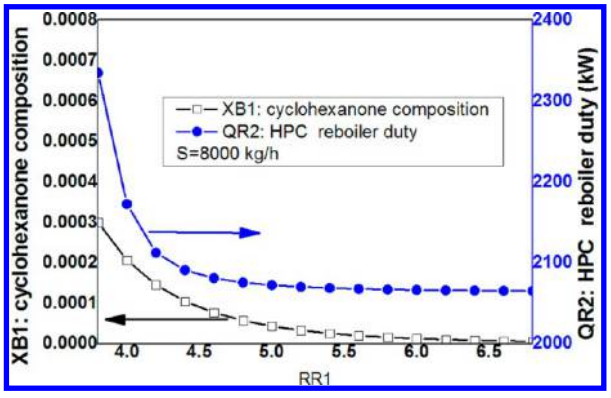

Figure 4. Effects of RR_1 on the cyclohexanone composition in the LPC bottoms stream and HPC reboiler duty with fixed S.

integrated process is slightly different from that of the partially heat-integrated process. In the fully heat-integrated process, RR_1 does not need to be optimized.

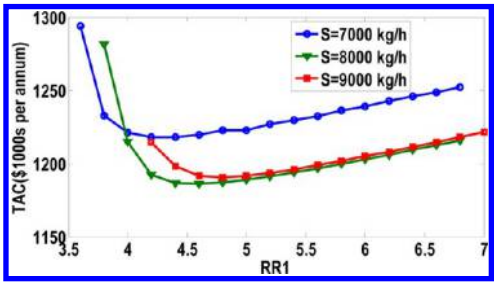

Figure 5. TAC plots versus RR_1 at various S values with N_1 = 35 and N_2 = 40.

The optimization for the fully heat-integrated process was started with several case studies. First, the effect of the number of stages N_1 in the LPC and recycle streamflow rate S are investigated. The TAC plots versus N_1 at various S with N_2 fixed at 40 are shown in Figure 8. It is obvious that the minimum TAC is achieved with N_1 = 24, N_2 = 40, and S = 9000 kg/h.

dx.doi.org/10.1021/ie400274d | Ind. Eng. Chem. Res. 2013, 52, 7836−7853

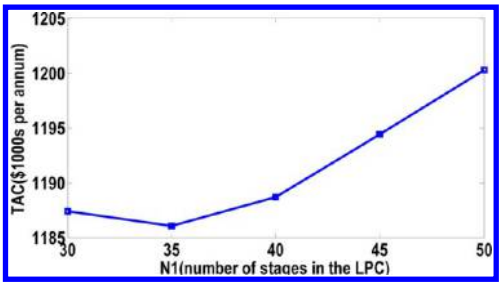

Figure 6. The effect of N_1 on TAC with N_2 fixed at 40.

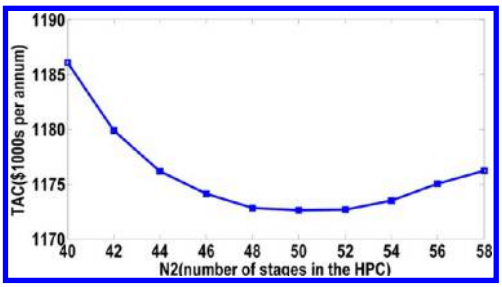

Figure 7. TAC plot versus N_2 with the optimum configurations of the LPC.

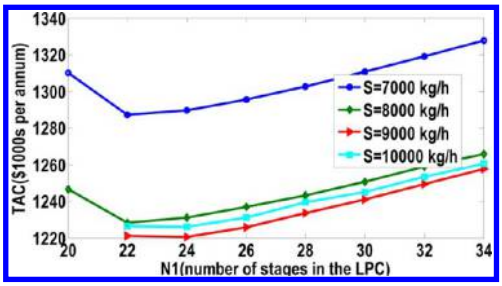

Figure 8. TAC plots versus N_1 at various S with N_2 = 40.

Then, the number of stages N_2 in the HPC is determined as it was done in the partially heat-integrated process. Several cases were carried out with N_1 = 24 and S = 9000 kg/h. The result indicates that the minimum TAC is $\$1.209 \times 10^6$ per annum with N_2 = 45.

2.3.3. Comparison between the Partially and Fully Heat-Integrated Processes. The optimized results of the partially and fully heat-integrated processes are listed in Table 3. The comparison confirms that the partially heat-integrated process is more economical, and it will be further optimized with the HPC operating pressure as an optimization variable.

Table 3. The Optimized Results of the Partially and Fully Heat-Integrated Processes with P_1 = 3 and P_2 = 200 kPa

parameters	partially heat-integrated process	fully heat-integrated process
N_1	35	24
N_2	50	45
S (kg/h) (optimum)	8000	9000
N_{F1}/N_{FR}	7/8	6/8
N_{F2}	20	21
RR_1/ RR_2	4.60/5.09	9.53/5.06
ID_1/ ID_2 (m)	1.58/1.37	1.90/1.37
QR_1/QC_1 (kW)	1058.5/−643.2	1663.2/−1209.0
QR_2/QC_2 (kW)	2009.4/−1672.5	2032.1/−1663.2
FCI ($1000s per annum)	1463.2	1572.2
TAC ($1000s per annum)	1172.6	1209.2

2.4. Selection of Optimum Operating Pressure in HPC.

The energy consumption is greatly affected by the operating pressure in the HPC. To determine the operating pressure in the HPC, alternatives operating at various pressures are compared based on TAC. The HPC operating at 180, 200, 220, and 240 kPa are studied for the partially heat-integrated flowsheet, separately. Since acetophenone dimerizes at 250 °C or above,[34] the operating pressure of the HPC that higher than 240 kPa will not be considered.

Table 4 shows the optimized results for various operating pressures. The results indicate that higher pressure makes the separation in the HPC easier. It is obvious that TAC decreases with increasing HPC pressure, and the case with operating pressure of 240 kPa in the HPC is the best.

Figure 9 gives the corresponding partially heat-integrated flowsheet with detailed stream information, heat duties, equipment sizes, and operating conditions.

3. CONTROL STRUCTURE DESIGN

The new pressure-swing distillation process is highly intercoupled and interacted through the bottom streams connecting the two columns and heat integration constraints. A disturbance occurring in one column can be easily transmitted into the other, resulting in interaction between the two columns, thus it is of significant importance to study the controllability of this new process. In this section, several control structures are proposed, and the dynamic performances of this new process are investigated. The optimal partially heat-integrated process is selected for the control study using Aspen Dynamics.

To convert the steady-state simulation to the dynamic one, the two column diameters are determined using "packing sizing" section. Reflux drums and column bases are sized to provide 5 min of holdup time when half full. Pumps are inserted to provide adequate pressure drops over valves and the valves are specified to have pressure drops of about 300 kPa with the valve half open at the design flow rate.[35]

3.1. Basic Temperature Control Structure.

In consideration of the widespread use of temperature in the chemical industry, temperature control was first considered. Figure 10 gives the temperature profiles in the two columns. According to the slope criterion proposed by Luyben,[32] stages 5 and 9 are selected as the temperature control locations for the LPC and HPC, respectively.

Wang,[5] Luyben[17,36,37] and Arifin et al.[26] have studied the temperature control structures for a conventional extractive distillation column. Yu[6] and Luyben[17,18] also presented several temperature control structures for conventional heat-integrated pressure-swing distillation processes. Their control structures provide effective disturbance rejection for both feed flow rate and feed composition changes. The new pressure-swing distillation process presented in this paper can be considered as a combination of the conventional extractive distillation and the conventional pressure-swing distillation. Thus a basic temperature control structure is developed for this new pressure-swing distillation process on the basis of the above control structures proposed by pioneers. Figure 11a illustrates this basic control structure and Figure 11b shows the controller faceplates.

(1) feed is flow-controlled (reverse acting);
(2) reflux drum levels of both columns are controlled by manipulating the corresponding distillates flow rate (direct acting);
(3) base level of the LPC is held by manipulating the bottom flow (direct acting), while the HPC base level is controlled with the makeup flow (reverse acting);

dx.doi.org/10.1021/ie400274d | Ind. Eng. Chem. Res. 2013, 52, 7836−7853

Table 4. Case Studies for the Global Economic Optimization of the Partially Heat-Integrated Process

parameters	P_2 = 180 kPa	P_2 = 200 kPa	P_2 = 220 kPa	P_2 = 240 kPa
N_1	35	35	35	35
N_2	50	50	50	55
S (kg/h) (optimum)	8000	8000	8000	8000
N_{F1}/N_{FR}	7/8	7/8	7/8	7/8
N_{F2}	20	20	21	23
RR_1/RR_2	4.65/5.27	4.60/5.09	4.45/4.95	4.35/4.78
ID_1/ID_2 (m)	1.58/1.40	1.58/1.37	1.57/1.35	1.56/1.30
QR_1/QC_1 (kW)	1064.3/−649.0	1058.5/−643.2	1041.2/−625.8	1029.6/−614.3
QR_2/QC_2 (kW)	2044.6/−1737.4	2009.4/−1672.5	1984.5/−1619.7	1951.8/−1560.8
FCI ($1000s per annum)	1479.5	1463.2	1447.4	1451.4
TAC ($1000s per annum)	1190.4	1172.6	1158.6	1147.8

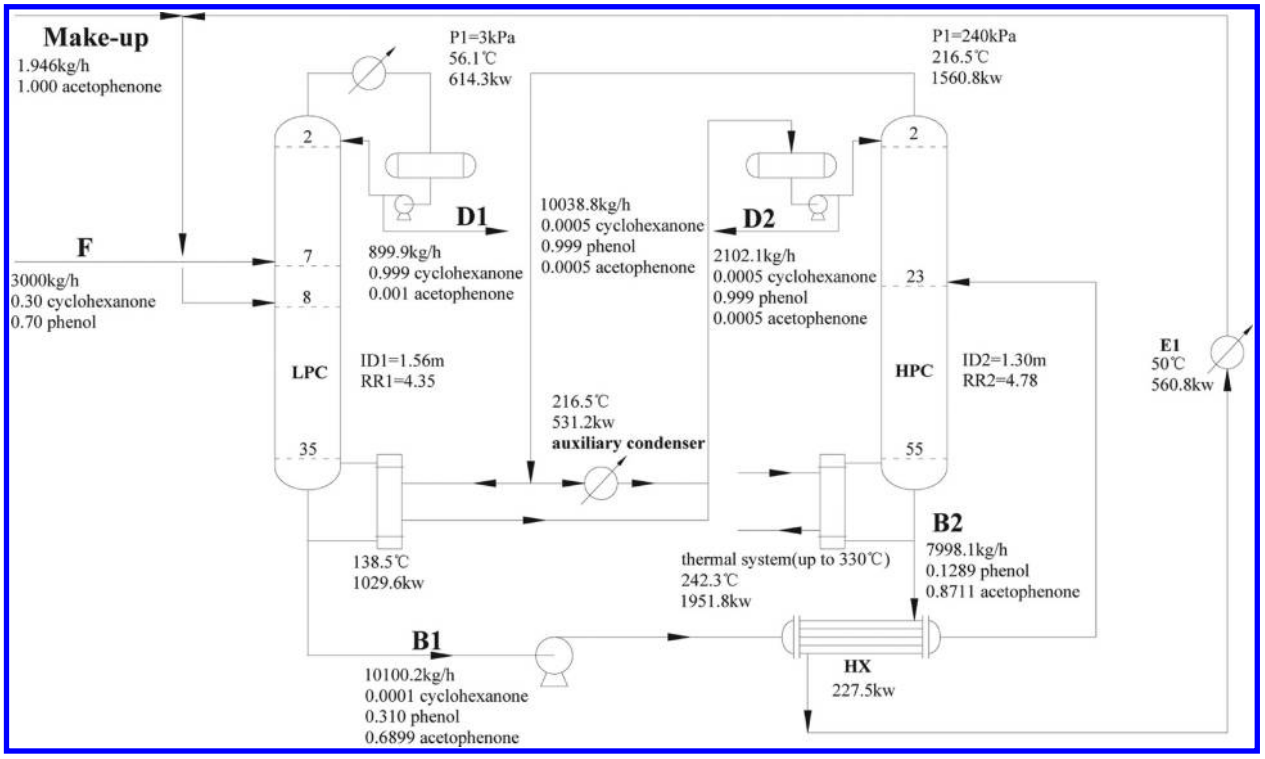

Figure 9. Flowsheet for the optimum new pressure-swing distillation process with partial heat integration.

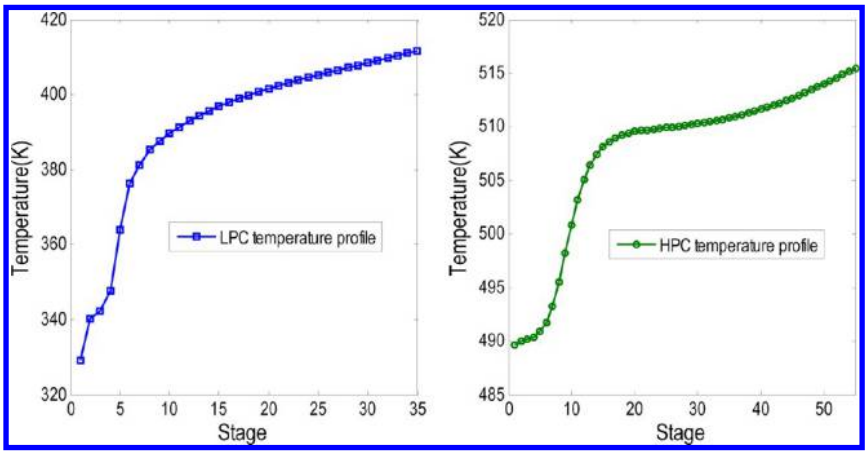

Figure 10. Temperature profiles in the LPC and HPC.

(4) the pressure of the LPC is controlled by manipulating the condenser heat removal rate (reverse acting), while the HPC pressure is held by manipulating the auxiliary condenser heat removal rate (reverse acting);

(5) the recycle streamflow rate is proportional to the feed flow rate;

(6) the HPC reboiler heat input is proportional to the feed molar flow rate;

dx.doi.org/10.1021/ie400274d | Ind. Eng. Chem. Res. 2013, 52, 7836−7853

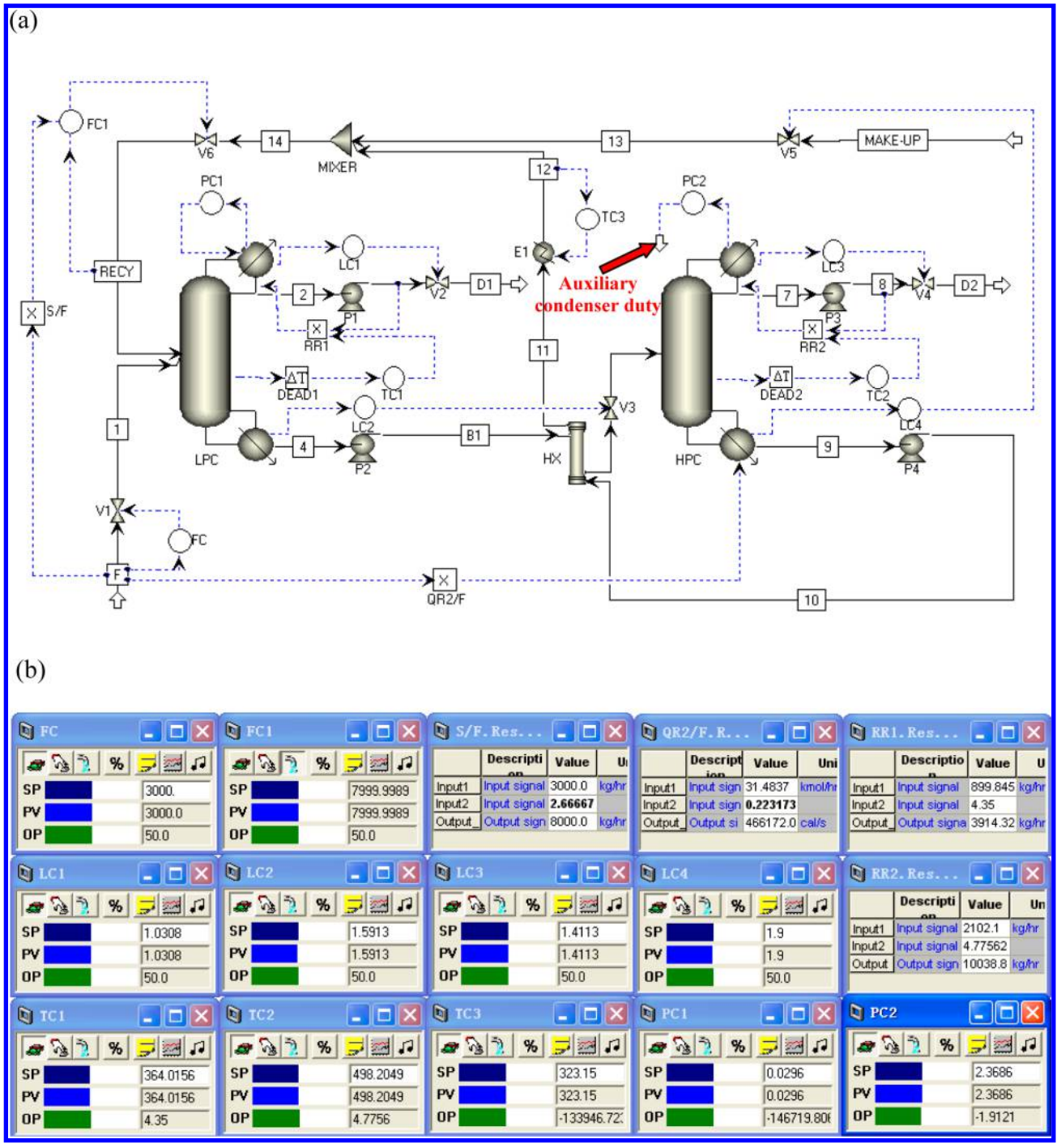

Figure 11. (a) Basic temperature control structure for the partially heat-integrated process. (b) Controller faceplates.

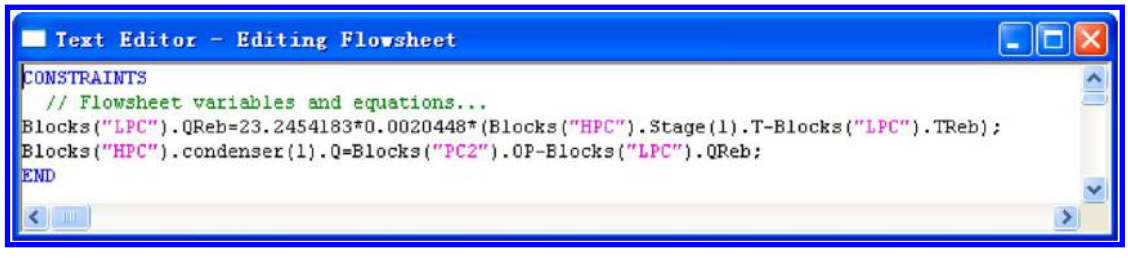

Figure 12. Flowsheet equations for the partial heat integration.

dx.doi.org/10.1021/ie400274d | Ind. Eng. Chem. Res. 2013, 52, 7836−7853

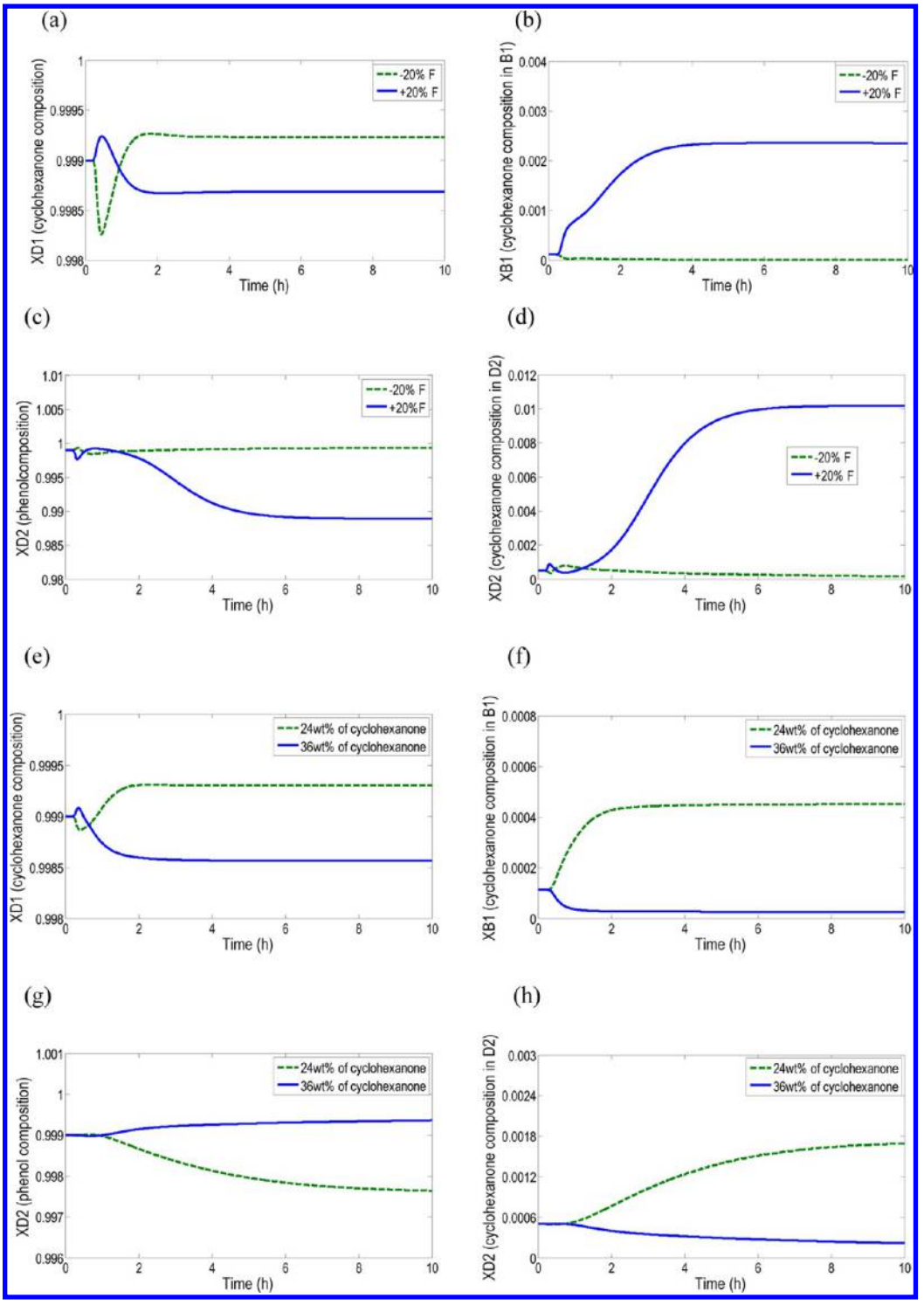

Figure 13. Dynamic responses for the basic temperature control structure: (a, b, c, and d) ±20% in feed flow rate (F), (e, f, g and h) ±20% in cyclohexanone composition. (x_D and x_B denote the mass fractions in the distillate and bottoms stream, respectively.).

(7) the recycle stream temperature is held by manipulating the cooler E1 heat removal rate (reverse acting);
(8) the temperatures, on stage 5 in the LPC and stage 9 in the HPC are controlled by manipulating the corresponding reflux ratio.

In these control loops, all flow controllers are PI with the normal settings: K_C = 0.5 and τ_I = 0.3 min. For the level controllers, only a proportional function is employed with gain equal to 2. The pressure controllers are PI with the default values in Aspen Dynamics. A 1-min deadtime is inserted in each temperature control loop for the columns. Relay-feedback tests for TC1 and TC2 are run to determine the ultimate gains and periods; TC3 is not tuned for the extremely fast response of cooler E1. Then, the Ziegler-Nichols tuning settings are applied to obtain the gain K_C and integral time constant τ_I. Details of tuning and setting are covered in Luyben's book.[35]

In this partially heat-integrated process, the heat input of the LPC is completely provided by the HPC with a combined

dx.doi.org/10.1021/ie400274d | Ind. Eng. Chem. Res. 2013, 52, 7836−7853

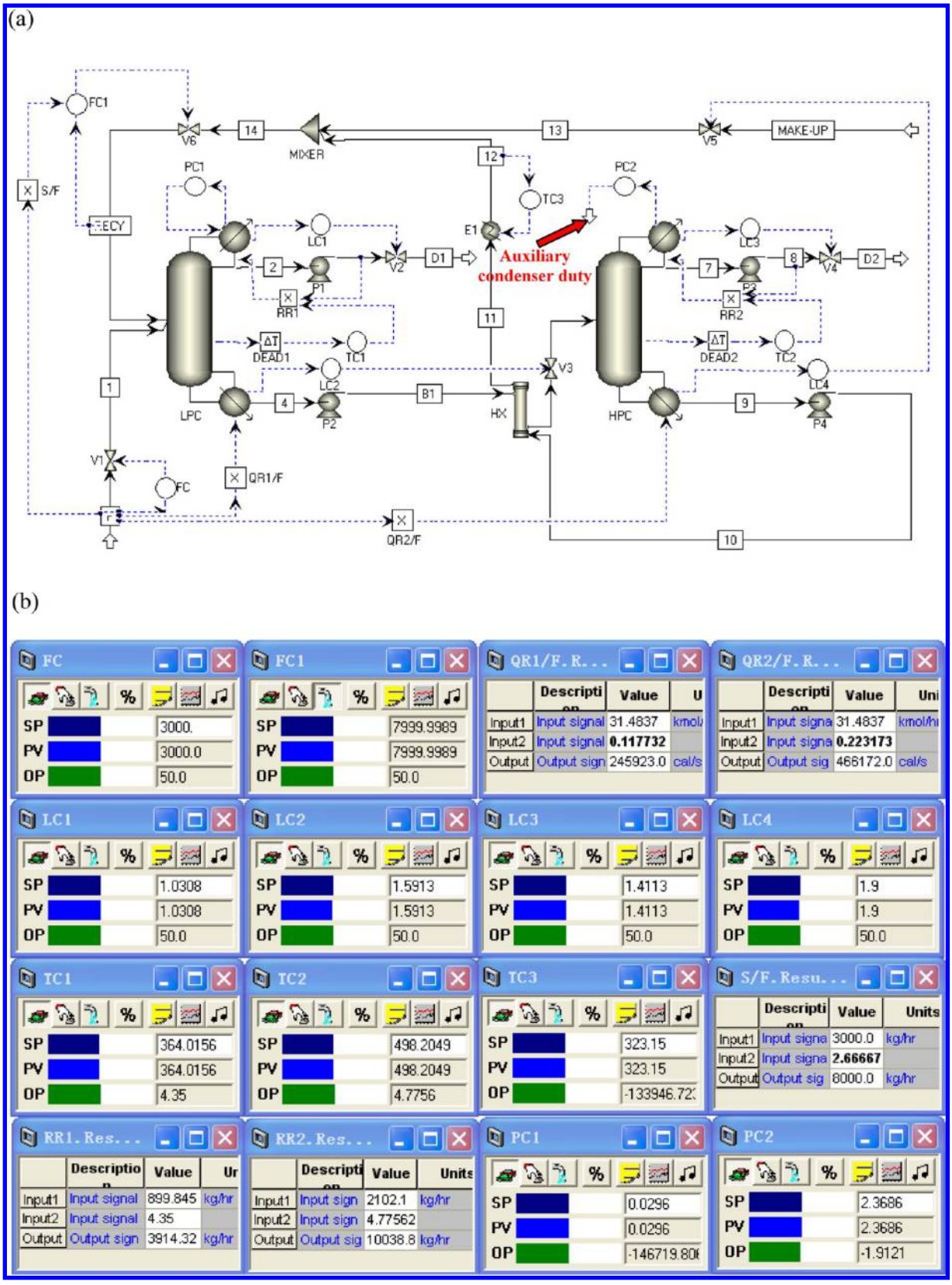

Figure 14. (a) Modified temperature control structure. (b) Controller faceplates.

reboiler/condenser. An auxiliary condenser is added to this process for removing the excessive heat of the HPC. The steady-state result gives a heat transfer area of 23.25 m^2 for the combined reboiler/condenser. The HPC condenser and the LPC reboiler duties are 5.619 and 3.707 GJ/h, respectively. Thus the auxiliary condenser heat removal rate is 5.619−3.707 = 1.912 GJ/h, the negative sign of this value is specified as the initial output signal of "PC2" controller.

dx.doi.org/10.1021/ie400274d | *Ind. Eng. Chem. Res.* 2013, 52, 7836−7853

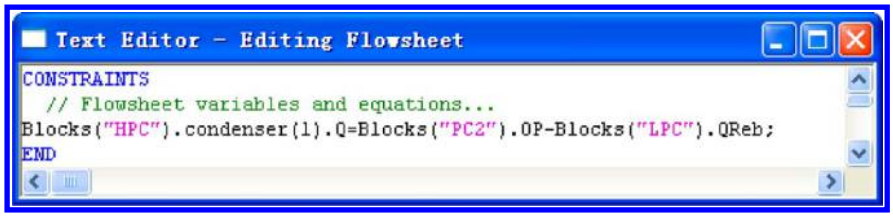

Figure 15. Flowsheet equation in this modified control structure.

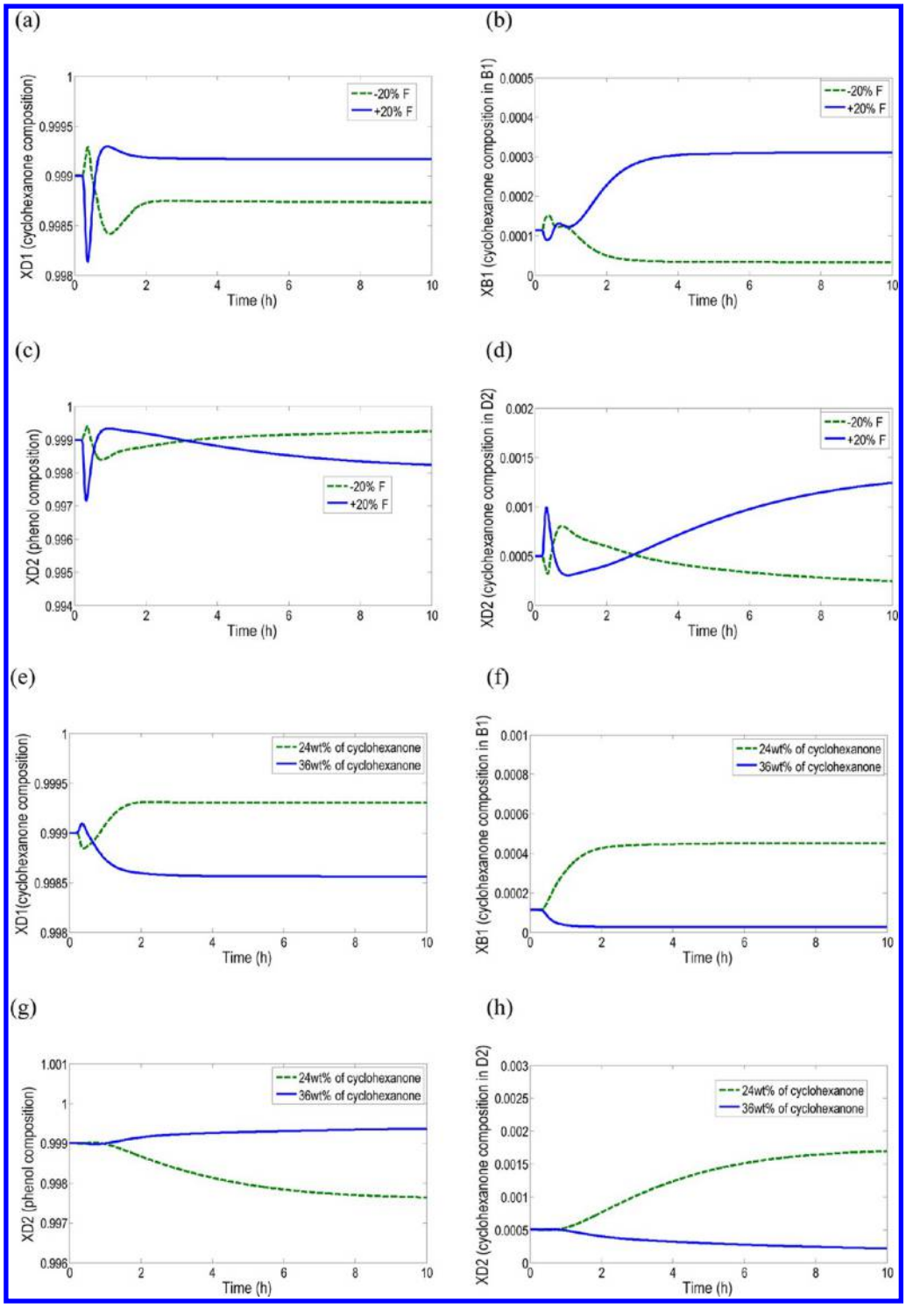

Figure 16. Dynamic responses for the modified temperature control structure: (a, b, c and d) ±20% in feed flow rate (F), (e, f, g and h) ±20% in cyclohexanone composition.

dx.doi.org/10.1021/ie400274d | *Ind. Eng. Chem. Res.* 2013, 52, 7836−7853

The "flowsheet equations" function is employed to achieve this partial heat integration. As shown in Figure 12, the HPC reboiler heat input is calculated using the first equation. The "PC2" controller is placed on automatic, and the HPC heat removal rate is calculated using the second equation.

The effectiveness of the basic temperature control structure is tested by making fresh feed flow rate and composition disturbances. For each case, a 20% step change is introduced to the fresh feed stream at $t = 0.2$ h. In this paper, unless otherwise specified, the dynamic responses for the negative and positive disturbances are represented by the dashed and solid lines, respectively. Figure 13 shows the dynamic responses for this basic temperature control structure.

As seen in Figure 13 panels a, b, c, and d, the mass purities of cyclohexanone product (D1) and phenol product (D2) can be closely maintained at their product specifications for the −20% feed flow rate disturbance, with the cyclohexanone impurities in B1 and D2 kept at a very low level. When the +20% flow rate disturbance occurs, the cyclohexanone product purity is still maintained close to its specification, while the phenol mass purity in D2 decreases to 98.90 wt %. The cyclohexanone composition in B1 rises from 0.01 to 0.24 wt % and the corresponding cyclohexanone impurity in D2 rises from 0.05 to 1.02 wt % at a new steady state. This is because the reboiler area of LPC is fixed and the heat transfer coefficient is assumed to be constant, therefore the heat input of LPC is mainly determined by the temperature difference between the HPC top and LPC base. Since the top product of the HPC is relatively pure phenol and the composition of the LPC bottom varies little, the temperature difference between the two ends is almost constant. So, the heat input of LPC is nearly constant. When +20% flow rate disturbance occurs, the LPC heat input is not adequate to produce sufficient vapor up to the top, resulting in more cyclohexanone escaping from the LPC bottoms. Then, the cyclohexanone that escapes from the LPC will mainly enter the HPC distillate and act as impurity.

The dynamic responses shown in Figure 13 panels e−h reveal that for the composition disturbances the cyclohexanone product purity can be closely maintained at its desired specification. However it takes more than 8 h for the phenol purity and cyclohexanone impurity in D2 to get to a new steady state. In addition, the cyclohexanone composition in B1 cannot be maintained at its initial value.

3.2. Modified Temperature Control Structure with QR_1/F Ratio. The basic temperature control structure could not provide effective disturbance rejection for the feed flow rate and feed composition changes, especially for the +20% feed flow rate change. The main reason is that the almost constant LPC heat input is not adequate to produce sufficient vapor up to the top when disturbances occur, resulting in more cyclohexanone escaping from the LPC bottoms to the HPC. Thus, a feedforward QR_1/F ratio (LPC reboiler duty/feed flow rate) is inserted on the basis of the basic control structure to improve the dynamic performances. Figure 14 illustrates this modified temperature control structure and controller faceplates. It should be noted that there is only one equation left in "flowsheet equation", as shown in Figure 15.

The effectiveness of this modified temperature control structure is tested with the same disturbances in our basic control structure and the dynamic responses are presented in Figure 16.

A comparison between the dynamic performances of the basic and modified temperature control structures is made. In both control structures, the cyclohexanone product purity can be closely maintained at its specification for the feed flow rate and composition disturbances. In this modified control structure, there is a significant improvement in the phenol product purity for +20% feed flow rate disturbance. It is note-worthy that the new steady-state phenol purity in D2 rises from 98.90 to 99.80 wt % with the cyclohexanone impurity reduced from 1.02 to 0.12 wt %. However, the cyclohexanone composition in B1 still cannot be maintained at its desired value. Furthermore, the dynamic responses of the phenol purity and cyclohexanone impurity in D2 for the same disturbances are quite similar in both control structure. For both control structures, it takes more than 8 h to get to a new steady state when the disturbances in composition occur. For the −20% cyclohexanone composition disturbance, the new steady-state phenol product purity is only 99.76 wt %, and the corresponding cyclohexanone impurity in D2 rises from 0.05 to 0.17 wt %.

The dynamic performances reveal that this new pressure-swing distillation process could not be perfectly controlled by these two temperature control structures and the reason for this will be discussed later. To achieve a robust control for the new process, we developed a third control structure.

3.3. Composition/Temperature Cascade Control Structure. The temperature control is widely used as a substitute to composition analysis in distillation control because of its high-reliability, little dynamic lag and low cost. However, the inherent drawbacks of temperature control are that it does not always correlate well with composition or may not always sufficiently be sensitive to variations in product composition.[38]

In the LPC, an extremely small amount of cyclohexanone would inevitably fall down to bottoms, and thereby enter the HPC. In the HPC, phenol, and acetophenone are the light and heavy key components, respectively, and the cyclohexanone/phenol azeotrope is considered as an intermediate nonkey component. This intermediate nonkey will accumulate at some place in the HPC. Figure 17 gives the steady-state composition profiles in the two columns.

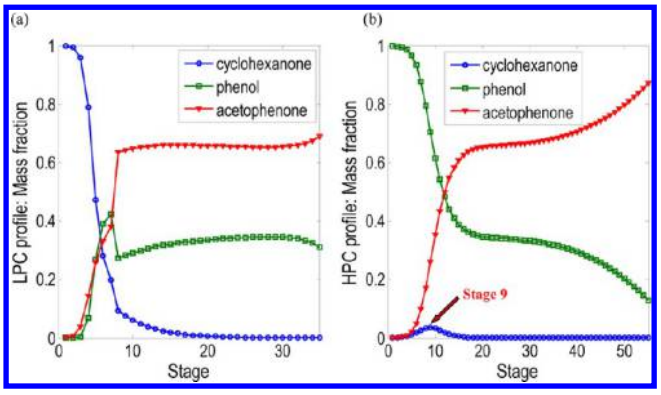

Figure 17. Composition profiles: (a) composition profiles in the LPC, and (b) profiles in the HPC.

As seen in Figure 17, cyclohexanone is accumulating at stage 9, and displays the highest mass fraction of 0.0356 in the HPC. In the previous two control structures, the temperature control location in the HPC is exactly at stage 9. Even a very small amount of unwanted cyclohexanone escaping from the LPC bottom could significantly affect the temperature profile in the HPC. The control temperature decreases with an increase in cyclohexanone concentration on stage 9. The temperature

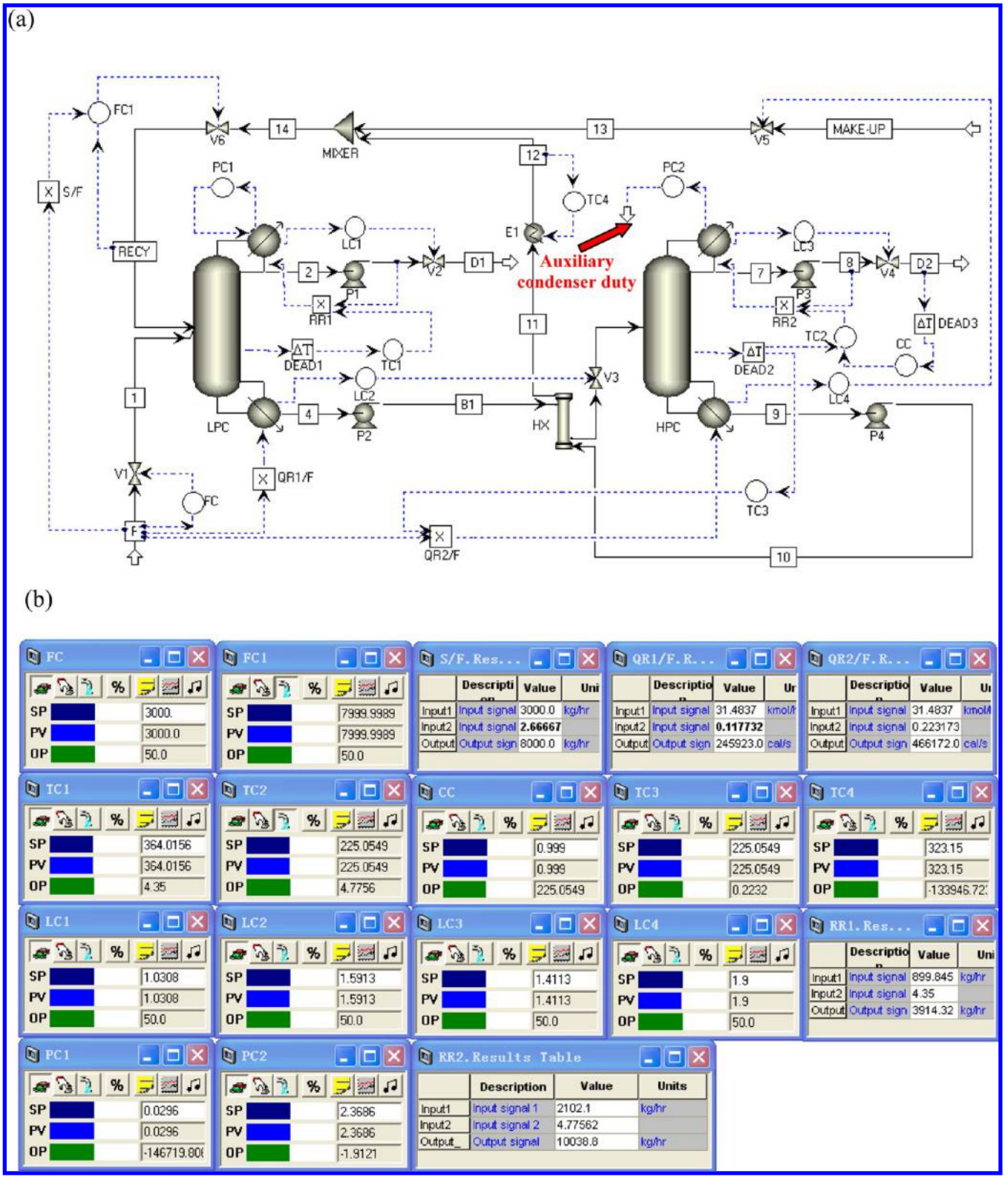

Figure 18. (a) The schematic diagram of the composition/temperature cascade control structure. (b) Controller faceplates.

controller will interpret the decrease to signal a rise in phenol concentration, and will subsequently counteract it (by cutting RR_2). This in turn induces cyclohexanone to rise up to the HPC distillate. In brief, the cyclohexanone/phenol nonkey would "fool" the temperature controller that is located at stage 9. This is the main reason why the two temperature control structures cannot perfectly control this new process.

There might be two ways to cope with the drawback of the two temperature control structures that is caused by the intermediate nonkey. One way is to strictly control the cyclohexanone composition in the LPC bottoms stream with a specific control loop. Then, we have developed several other control structures in which this cyclohexanone composition is strictly controlled with a composition control loop. However, all of these control structures fail to stabilize

dx.doi.org/10.1021/ie400274d | Ind. Eng. Chem. Res. 2013, 52, 7836−7853

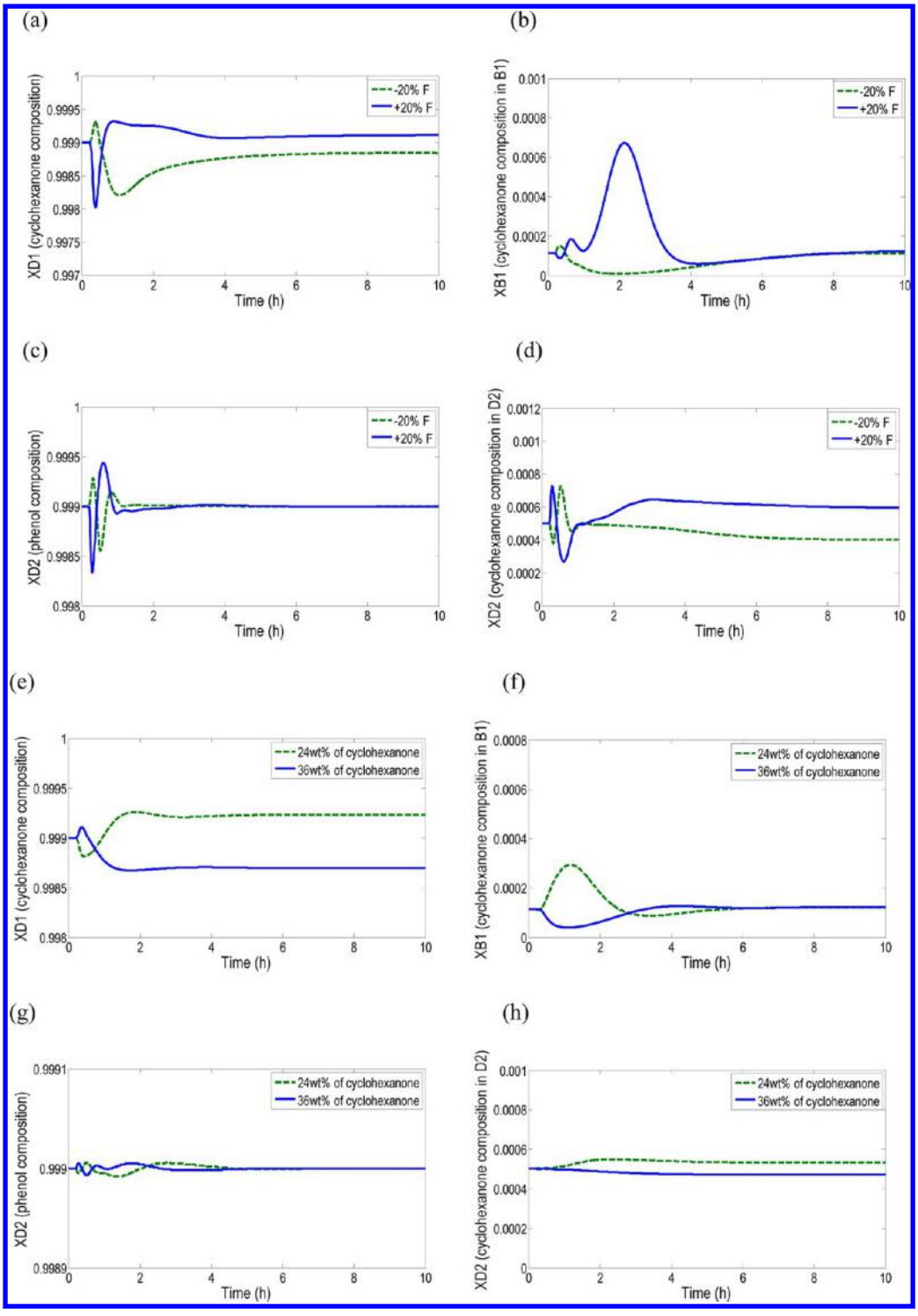

Figure 19. Dynamic responses for the composition/temperature control structure: (a, b, c and d) ±20% in feed flow rate (F), (e, f, g and h) ±20% in cyclohexanone composition.

this new process. The other potential way is to develop a control loop that can eliminate the influence of cyclohexanone on the controllability of the HPC. Since the two columns are interacting with each other, a tighter control for the HPC would in turn favor greatly the control of the LPC. Thus, a composition/temperature cascade control is proposed. Figure 18 gives the schematic diagram of this cascade control structure and controller faceplates.

In the composition/temperature cascade control structure, phenol concentration in D2 is measured, and then transmitted to a composition controller CC as the input signal. The output signal of CC is the set point signal of temperature controller TC2. Controller CC is direct-acting with a 5-min deadtime. The QR_2/F ratio is adjusted by the temperature on stage 9 of the HPC to reduce the settling time. It should be noted that temperature controller TC1, TC2, and TC3 are tuned as normal, while the composition controller CC is tuned with TC2 on cascade.

The dynamic performances for this composition/temperature cascade control structure are demonstrated in Figures 19, 20, and 21.

dx.doi.org/10.1021/ie400274d | Ind. Eng. Chem. Res. 2013, 52, 7836−7853

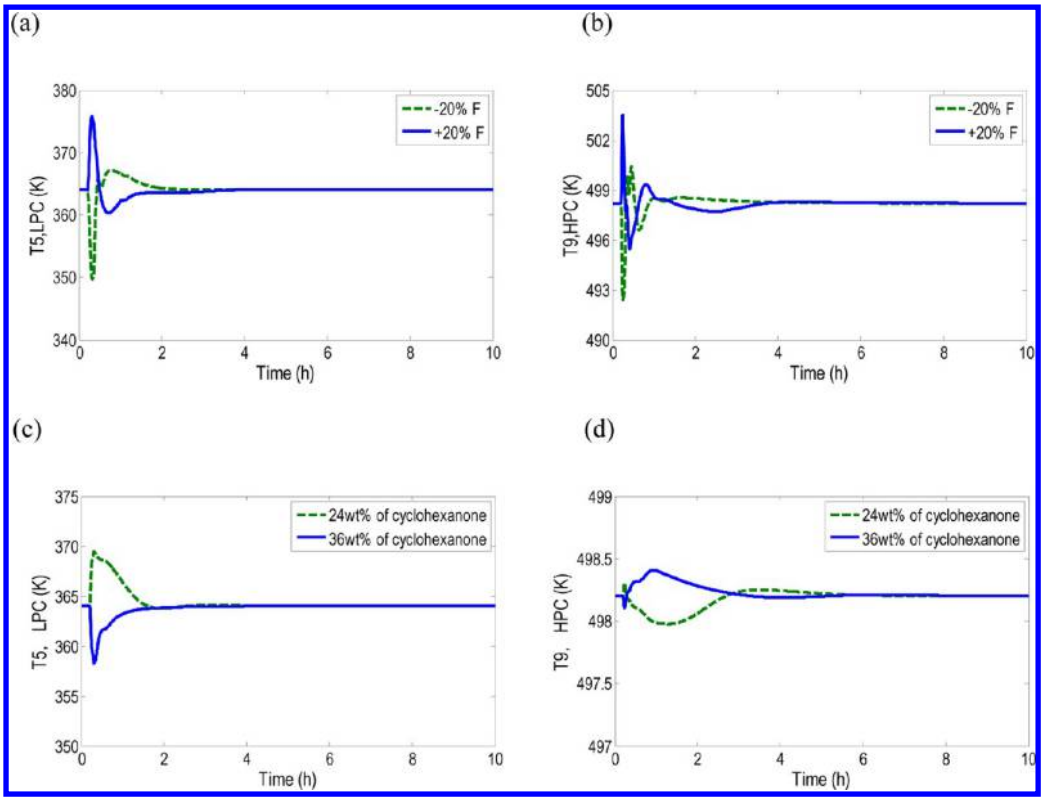

Figure 20. Dynamic responses of two controlled temperatures: (a, b) ±20% in feed flow rate (F), (c, d) ±20% in cyclohexanone composition.

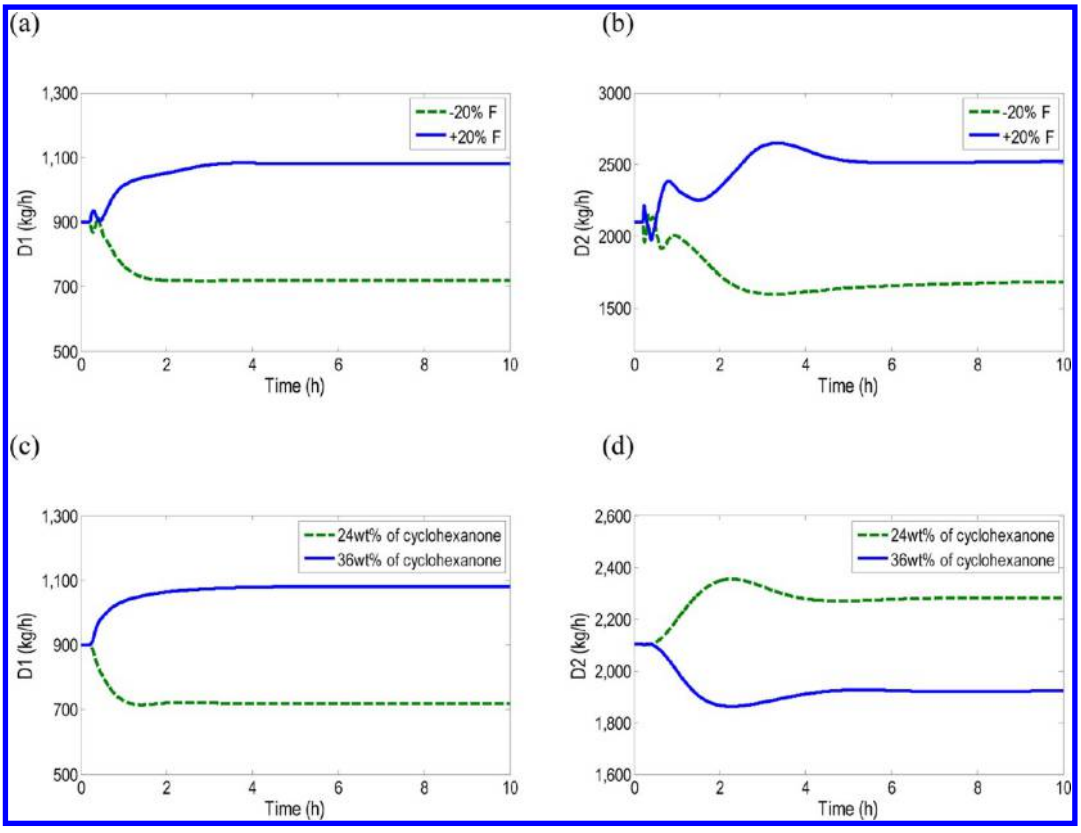

Figure 21. Dynamic responses of two product flow rates: (a, b) ±20% in feed flow rate (F), (c, d) ±20% in cyclohexanone composition.

As seen in Figure 19, the dynamic response of the cyclohexanone product purity is almost the same with that in the modified control structure, while a significant improvement is gained in the response of cyclohexanone composition in the LPC bottoms stream B1. The cyclohexanone composition in B1 can be easily brought back to its initial level within 8 h. For both feed flow rate

dx.doi.org/10.1021/ie400274d | *Ind. Eng. Chem. Res.* 2013, 52, 7836−7853

and composition disturbances, the phenol product purity is maintained at its specification with a negligible deviation, and the corresponding cyclohexanone impurity is held extremely close to its initial level (0.05 wt %). Figure 20 shows that the controlled temperatures are brought back to their initial set points. Figure 21 reveals that the flow rates of the two product can be brought to their desired specifications. All these results indicate that the drawbacks of the temperature control structures can be fairly well cured by this composition/temperature control structure and a robust control is achieved for this new process.

4. CONCLUSION

A new pressure-swing distillation for separating pressure-insensitive maximum boiling phenol/cyclohexanone azeotrope via the introduction of acetophenone is developed with the aid of Aspen Plus. Both fully and partially heat-integrated configurations are explored, and it is revealed that the partially heat-integrated process is more economical than the fully heat-integrated one in terms of TAC. Accordingly, the optimum design of the partially heat-integrated process is obtained.

Three control structures are proposed to stabilize the optimum partially heat-integrated process. The basic temperature control structure with a fixed controlled temperature could not maintain the phenol product quality for large disturbances, especially for +20% feed flow rate disturbance. Then, a modified temperature control structure with a feedforward QR_1/F ratio is further explored to improve the dynamic responses of the phenol product purity, but the inherent drawbacks caused by the intermediate nonkey still cannot be overcome. Hence, a composition/temperature cascade control scheme has been proposed and a robust control of this process is achieved with the inherent drawbacks well cured.

The results reveal that this new pressure-swing distillation process is worth considering during the conceptual design stage of the distillation processes for separating pressure-insensitive maximum boiling azeotropes.

AUTHOR INFORMATION

Corresponding Author

*Tel.: +86 022-27892145. Fax: +86 022-27404440. E-mail: cjxu@tju.edu.cn.

Notes

The authors declare no competing financial interest.

ACKNOWLEDGMENTS

Weisong Li and coauthors are grateful to Dr. Chi-Wing Tsang for his assistance.

NOMENCLATURE

B_1 = bottom flow rate from LPC column (kg/h)
B_2 = bottom flow rate from HPC column (kg/h)
D_1 = distillate flow rate from LPC column (kg/h)
D_2 = distillate flow rate from HPC column (kg/h)
HPC = high pressure column
ID_1 = internal diameter for the LPC column (m)
ID_2 = internal diameter for the HPC column (m)
LPC = low pressure column
N_1 = number of stages in the LPC
N_2 = number of stages in the HPC
N_{F1} = feeding location for the fresh feed
N_{FR} = feeding location for the recycle stream
N_{F2} = feeding location for the feed of the HPC
QR_1 = reboiler duty of the LPC (kW)
QR_2 = reboiler duty of the HPC (kW)
RR_1 = reflux ratio of the LPC
RR_2 = reflux ratio of the HPC
TAC = total annual cost (× $1000s per annum)
$T_{n,LPC}$ = temperature on stage n in the LPC (K)
$T_{n,HPC}$ = temperature on stage n in the HPC (K)

REFERENCES

(1) Yadav, G. D.; Asthana, N. S. Selective Decomposition of Cumene Hydroperoxide into Phenol and Acetone by a Novel Cesium Substituted Heteropolyacid on Clay. *Appl. Catal.* **2003**, *244*, 341−357.
(2) Langley, P. E. Process for the Production of Phenol and Acetone. U.S. Patent 4310712, January 12, 1982.
(3) Aoki, Y.; Sakaguchi, S.; Ishii, Y. One-pot Synthesis of Phenol and Cyclohexanone from Cyclohexylbenzene Catalyzed by *N*-hydroxyphethalimide (NHPI). *Tetrahedron Lett.* **2005**, *61*, 5219−5222.
(4) Hudson, P. S. Process for Production of Phenol and Cyclohexanone. U.S. Patent 4021490, May 3, 1977.
(5) Wang, Q.; Yu, B.; Xu, C. Design and Control of Distillation System for Methylal/Methanol Separation. Part 1: Extractive Distillation Using DMF as an Entrainer. *Ind. Eng. Chem. Res.* **2012**, *51*, 1281−1292.
(6) Yu, B.; Wang, Q.; Xu, C. Design and Control of Distillation System for Methylal/Methanol Separation. Part 2: Pressure Swing Distillation with Full Heat Integration. *Ind. Eng. Chem. Res.* **2012**, *51*, 1293−1310.
(7) Ligero, E. L.; Ravagnani, T. M. K. Dehydration of Ethanol with Salt Extractive Distillation—A Comparative Analysis between Processes with Salt Recovery. *Chem. Eng. Pro.* **2003**, *42*, 543−552.
(8) Lang, P.; Modla, G.; Benadda, G.; Lelkes, Z. Homoazeotropic Distillation of Maximum Azeotropes in a Batch Rectifier with Continuous Entrainer Feeding I. Feasibility Studies. *Com. Chem. Eng.* **2000**, *24*, 1665−1671.
(9) Lang, P.; Modla, G.; Kotai, B.; Lelkes, Z.; Moszkowicz, P. Homoazeotropic Distillation of Maximum Azeotropes in a Batch Rectifier with Continuous Entrainer Feeding II. Rigorous Simulation Results. *Com. Chem. Eng.* **2000**, *24*, 1429−1435.
(10) Lelkes, Z.; Rev, E.; Steger, C.; Fonyo, Z. Batch Extractive Distillation of Maximal Azeotrope with Middle Boiling Entrainer. *AIChE J.* **2002**, *48*, 2524−2536.
(11) Kotai, B.; Lang, P.; Balazs, T. Separation of Maximum Azeotropes in a Middle Vessel Column. *IChemE Symp. Ser.* **2006**, 699−708.
(12) Kotai, B.; Lang, P.; Modla, G. Batch Extractive Distillation as a Hybrid Process: Separation of Minimum Boiling Azeotropes. *Chem. Eng. Sci.* **2007**, *62*, 6816−6826.
(13) Repke, J. U.; Klein, A.; Bogle, D.; Wozny, G. Pressure Swing Batch Distillation for Homogenous Azeotropic Separation. *Chem. Eng. Res. Des.* **2007**, *85*, 492−501.
(14) Modla, G.; Lang, P. Feasibility of New Pressure Swing Batch Distillation Methods. *Chem. Eng. Sci.* **2008**, *63*, 2856−2874.
(15) Modla, G.; Lang, P.; Kopasz, A. Entrainer Selection for Pressure Swing Batch Distillation. *ESCAPE-18*; Elsevier B. V.: Amsterdam, 2008, ISBN 978-0-444-53228-2.
(16) Modla, G.; Lang, P.; Denes, F. Feasibility of Separation of Ternary Mixtures by Pressure Swing Batch Distillation. *Chem. Eng. Sci.* **2010**, *65*, 870−881.
(17) Luyben, W. L. Comparison of Extractive Distillation and Pressure-Swing Distillation for Acetone−Methanol Separation. *Ind. Eng. Chem. Res.* **2008**, *47*, 2696−2707.
(18) Luyben, W. L. Design and Control of a Fully Heat-Integrated Pressure-Swing Azeotropic Distillation System. *Ind. Eng. Chem. Res.* **2008**, *47*, 2681−2695.
(19) Muñoz, R.; Montón, J. B.; Burguet, M. C.; Torre, J. de la. Separation of Isobutyl Alcohol and Isobutyl Acetate by Extractive Distillation and Pressure-Swing Distillation: Simulation and Optimization. *Sep. Purif. Technol.* **2006**, *50*, 175−183.
(20) Knapp, J. P.; Doherty, M. F. A New Pressure-Swing-Distillation Process for Separating Homogeneous Azeotropic Mixtures. *Ind. Eng. Chem. Res.* **1992**, *31*, 346−357.

(21) Foucher, E. R.; Doherty, M. F.; Malone, M. F. Automatic Screening of Entrainers for Homogeneous Azeotropic Distillation. *Ind. Eng. Chem. Res.* **1991**, *30*, 760−772.
(22) Braam, van D.; Izak, N. Design of Solvents for Extractive Distillation. *Ind. Eng. Chem. Res.* **2000**, *39*, 1423−1429.
(23) Wu, L.; Chang, W.; Guan, G. Extractants Design Based on an Improved Genetic Algorithm. *Ind. Eng. Chem. Res.* **2007**, *46*, 1254−1258.
(24) Seider, W. D.; Seader, J. D.; Lewin, D. R. *Product and Processes Design Principles*; John Wiley & Sons, Inc: New York, 2004; pp 6−13.
(25) Douglas, J. M. *Conceptual Design of Chemical Processes*; McGraw Hill: New York, 1998; pp 568−577.
(26) Arifin, S.; Chien, I. L. Design and Control of an Isopropyl Alcohol Dehydration Process via Extractive Distillation Using Dimethyl Sulfoxide as an Entrainer. *Ind. Eng. Chem. Res.* **2008**, *47*, 790−803.
(27) Gmehling, Jürgen; Menke, Jochen; Krafczyk, Jörg; Fischer, Kai. Azeotropic Data. Wiley-VCH: Weinheim, Germany, 2004; pp 657−665.
(28) Gmehling, J.; Onken, U.; Weidlich, U. Vapor−Liquid Equilibrium Data Collection. DecHEMA: Frankfurt am Main, 1999.
(29) Giles, N. F.; Wilson, G. M. Vapor−Liquid Equilibria on Seven Binary Systems: Ethylene Oxide+2-Methylpropane; Acetophenone +Phenol; cis-1,3-Dichloropropene+1,2-Dichloropropane; 1,5-hexadiene+Allyl Chloride; Isopropyl Acetate+Acetonitrile; Vinyl Chloride +Methyl Chloride; and 1,4-Butanediol+γ-Butyrolactone. *J. Chem. Eng. Data* **2006**, *51*, 1954−1962.
(30) Knapp, J. P.; Doherty, M. F. Thermal Integration of Homogeneous Azeotropic Distillation Sequences. *AIChE J.* **1990**, *36*, 969−984.
(31) Zhang, P.; Liu, C.; Wang, L.; Tang, Z.; Yu, G. Performance of Structured Packing in High Pressure Distillation. *Chin. J. Chem. Eng.* **2002**, *10*, 635−638.
(32) Luyben, W. L. *Distillation Design and Control Using Aspen Simulation*; Wiley & Sons, Inc: NJ, 2006; pp 87−97.
(33) Turton, R.; Bailie, R. C.; Whiting, W. B.; Shaeiwitz, J. A. *Analysis, Synthesis and Design of Chemical Processes*; Prentice Hall: Upper Saddle River, NJ, 2009.
(34) Black, J. R.; Payne, L. W.; Unger, P. E. Recovery of Acetophenone during the Production of Phenol. U.S. Patent 0029239, February 2, 2012.
(35) Luyben, W. L. *Plantwide Dynamic Simulators in Chemical Processing and Control*; Marcel Dekker: New York, 2002; pp 11−24.
(36) Luyben, W. L. Plantwide Control of an Isopropyl Alcohol Dehydration Process. *AIChE J.* **2006**, *52*, 2290−2296.
(37) Luyben, W. L. Comparison of Pressure-Swing and Extractive-Distillation Methods for Methanol-Recovery Systems in the TAME Reactive-Distillation Process. *Ind. Eng. Chem. Res.* **2005**, *44*, 5715−5725.
(38) Kister, H. Z. *Distillation Operation*; McGraw Hill: New York, 1989; pp 545−561.